

Vertical wake deflection for offshore floating wind turbines by differential ballast control

Emmanouil M Nanos¹, Stefano Letizia², Daniel J Barreiro Clemente¹, Chengyu Wang¹, Mario Rotea², Valerio I Iungo² and Carlo L Bottasso¹

¹Wind Energy Institute, Technische Universität München, Garching bei München, Germany.

²Department of Mechanical Engineering, University of Texas at Dallas, Dallas, USA.

E-mail: em.nanos@tum.de

Abstract. This paper discusses the idea of vertical wake deflection for offshore wind turbines using active ballast control. First, the concept of active ballast control for changing the attitude of an offshore wind energy semi-submersible platform is presented and briefly explored. Next, the influence of vertical wake deflection on the wake behavior and power production of a cluster of two wind turbines is studied through wind tunnel experiments and LES simulations. Results show that vertical deflection changes substantially the wake characteristics and affects the inflow at a downstream wind turbine in terms of available kinetic energy and turbulence intensity. For the most favorable case considered here, the cluster power was increased by approximately 8%.

1. Introduction

Power production from wind is typically organized in clusters of wind turbines. It is well known that wake interactions among turbines have adverse effects on their performance and life expectancy. For typical offshore conditions, wakes persist many diameters downstream of the rotor because of the low turbulence of the atmospheric boundary layer. The main remedies against these effects proposed so far are based on either changing the wake characteristics (velocity deficit, recovery rate) by altering statically/dynamically the induction factor, or redirecting its path [1]. Yaw-based lateral wake redirection has shown good potential and does not require any radical hardware modification, since most wind turbines are already equipped with active yaw control; therefore, it has been at the center of attention of the recent literature. On the other end, studies on vertical deflection are significantly less common since the application of that method would require significant design modifications. Nevertheless, there are some studies [2, 3] that have addressed the topic using CFD with promising results.

While lateral wake redirection is effective because it reduces the interaction of downstream rotors by changing the wake path, deflecting the wake vertically can have multiple effects. First, similarly to lateral redirection techniques, it translates the wake out of the rotor area of a downstream machine. Second, it enhances wake recovery by either deflecting the wake upwards to a higher momentum flow area, or by deflecting the wake downwards, where the interaction with the sea surface could lead to a faster collapse of the wake coherent structures and enhance mixing.

Floating wind energy, which is growing fast, may provide a favorable environment for



implementing vertical wake control. In fact, some of the floating concepts incorporate water ballast control systems to modify the attitude of the floating platform [4]. This system could be used to tilt the structure (including the wind turbine) without the necessity of introducing additional mechanisms. However, ballast control is a relatively slow degree of freedom and it is also potentially expensive from an energetic point of view. Therefore, this control method cannot be treated as yaw, which can be changed relatively rapidly to follow wind direction changes. The two control techniques could be used in synergy: lateral deflection could be used for faster time scales, while vertical deflection on slower ones. This combined approach opens up various opportunities for optimization. Although this is a very interesting topic, the present paper has a narrower scope. Section 2 considers several offshore foundation concepts and presents some preliminary calculations on ballast control for vertical wake deflection. In section 3, the effect of a tilted rotor on the wake is discussed, while section 4 presents the most significant conclusions as well as an outlook on future work.

2. Tilt control of floating wind turbines

2.1. Brief review of floating foundation concepts

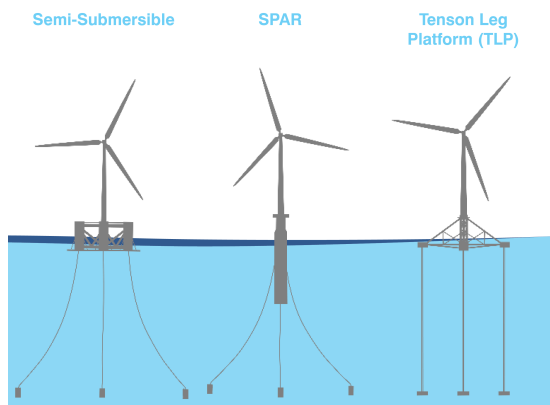


Figure 1: Floating foundation concepts (figure credit of FWE [5]).

Over the last years and three main concepts of floating wind turbine foundations have been proposed (Fig. 1):

- Semi-submersible
- Spar type
- Tension leg platform (TLP)

The spar foundation provides stability by keeping the center of buoyancy well above the center of gravity, thus creating a large recovering moment whenever the structure pitches away from the vertical position. In the TLP case, stability is provided by the mooring system whose legs are kept in a state of tension by buoyancy forces. The semi-submersible platform consists usually of three or four columns, with the turbine fixed on either one of them or at the center of the structure. Here, the hydrodynamic stability is achieved mainly through the large wetted surface. There are several advantages of the semi-submersible platform, which make it at present the most popular concept [6].

This configuration is of particular interest for the focus of this paper, because the ballast stored in each of the columns can be moved from column to column, changing the position of the center

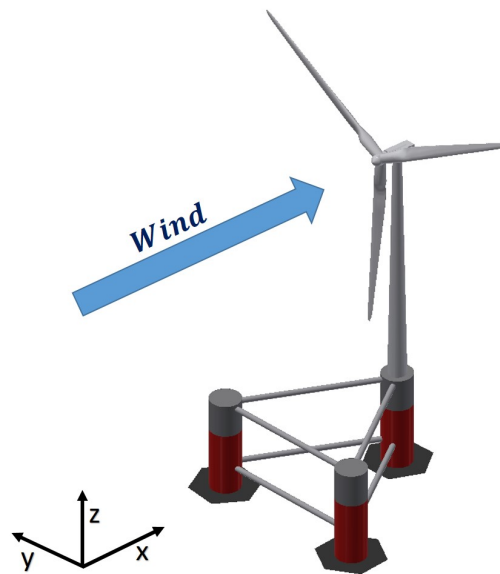


Figure 2: Sketch of the conceptual semi-submersible platform and wind turbine used in this study.

of gravity and forcing the platform to a desired pitch attitude. Active ballast control systems are already present in semi-submersible platforms used in the oil industry and are already included in offshore wind conceptual designs, where its purpose is mainly to counteract the pitching moment created by the thrust force of the rotor. Therefore, one may think of exploiting this system to perform the additional task of vertical wake deflection.

2.2. Study case

In this section, preliminary calculations of a semi-submersible platform are performed for an initial verification of the feasibility of the concept. To this purpose, a semi-submersible platform and its supported wind turbine are assumed and sketched in Fig. 2. The semi-submersible platform has three floating columns and the turbine is placed at the top of one of them, a concept that was introduced in WindFloat [4] and served as a basis for the platform dimensions and weight assumed in this article. The wind turbine is a generic 5 MW machine.

In this preliminary analysis, some major assumptions are made: the center of flotation (CF) is kept fixed as the platform pitches around it, the forces exerted by the mooring lines are neglected, the wind is steady and there is no wave excitation. Furthermore, in this study forward pitch of the platform generates a negative tilt angle, which deflects the wake towards the ground. Conversely, a backward pitch of the platform generates a positive tilt angle of the rotor, which deflects the wake towards the sky. It is further assumed that the platform has initially the right distribution of ballast among its columns, so that it is completely horizontal when there is no wind and the turbine is not operating. When the wind turbine operates at rated wind speed producing 700 kN of thrust, and no further action is taken by the ballast system, the platform will pitch around its center of flotation by approximately 4.5° (position A in Fig. 3). If this is added to the rotor pre-tilt, which is usually around 5° , the cumulative backward tilt of the rotor reaches almost 10° . At this point, the active ballast control could be used to bring the rotor in a completely perpendicular-to-the-wind attitude (position B), thus increasing the power in a greedy manner. Alternatively, ballast could be used for tilting the rotor to an angle that benefits

Table 1: Basic characteristics of the platform and the wind turbine used for the calculations.

| Platform characteristics | |
|---------------------------------|-----------|
| Column length | 35 m |
| Column diameter | 10.7 m |
| Column to column distance | 56.4 m |
| Total weight | 4000 tons |
| Turbine characteristics | |
| Total weight | 700 tons |
| Hub height | 88 m |
| Rated thrust | 700 kN |

the wind farm. For instance, to deflect the wake towards the sea surface the platform should be pitched forward. To achieve a -10° rotor tilt, the platform should be pitched by about 20° (position C in the figure). Similarly, to deflect the wake towards the sky, the platform should be pitched backwards. For example, to reach a rotor tilt of 15° , one would have to pitch the platform by another 5° (position D in the figure). In all cases, ballast has to be redistributed among the three columns in order to move the center of gravity of the structure and create a pitching a moment around the CF until the platform finds its equilibrium in the desired position. In the example presented here, given the platform weight, shape and dimensions (Table 1) and under the aforementioned assumptions, one can apply the hydrostatic equations and calculate the necessary ballast mass that has to be moved in order to achieve a specific pitch of the platform. In the present case, it was found that the necessary ballast movement is $45 \text{ m}^3/\text{deg}$. Taking into consideration the piping of the ballast system, achieving the hypothetical rotations of the platform described above would require 900 m^3 of water and 20 minutes to move from position A to position C. Similarly, it would require 225 m^3 and 5 minutes for moving from A to D. It is clear from this discussion that, with the configuration chosen for this specific study case, upward wake deflection requires less time and can reach higher rotor-wind misalignment angles than downward wake deflection. The exact mechanics of the tilting process, as well as the optimum configuration (type of turbine and platform) for implementing vertical wake control requires, undoubtedly, further investigation.

3. Effects of tilt

3.1. Wind tunnel tests

To characterize the effects of vertical wake deflection, experiments were conducted in the atmospheric boundary layer wind tunnel (BLAST) at the University of Texas at Dallas (UTD). A moderately turbulent inflow was achieved with the use of spires and roughness elements. The incoming wind followed the power law with an exponent of $a = 0.2$, while wind speed and turbulence intensity at hub height were $u = 10.4 \text{ m/s}$ and $I_u = 8.5\%$, respectively. This inflow profile is very close to a typical offshore condition [7]. The scaled model [8] is a 0.6 m turbine that, given the wind tunnel dimensions, resulted in a 4.8% blockage ratio. Two wind turbines were installed in the test section. The turbines were one behind the other, aligned and 5D apart, and they were operating at prescribed blade pitch angle and tip speed ratio of $\beta = 0^\circ$ and $\lambda = 7$, which correspond to the models optimum operating point (Region 2). Even though 5D is not a typical offshore longitudinal spacing, this distance was chosen for other technical reasons. Besides, even with this spacing it is still possible to identify trends, while this experimental data

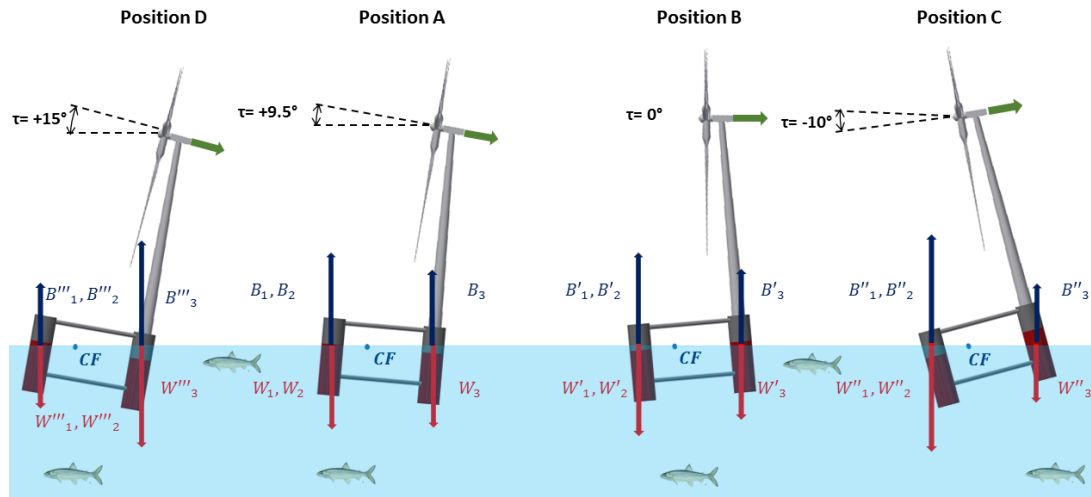


Figure 3: Schematic representation of the platform positions. For each position the forces that were taken into account for the attitude analysis are also shown.

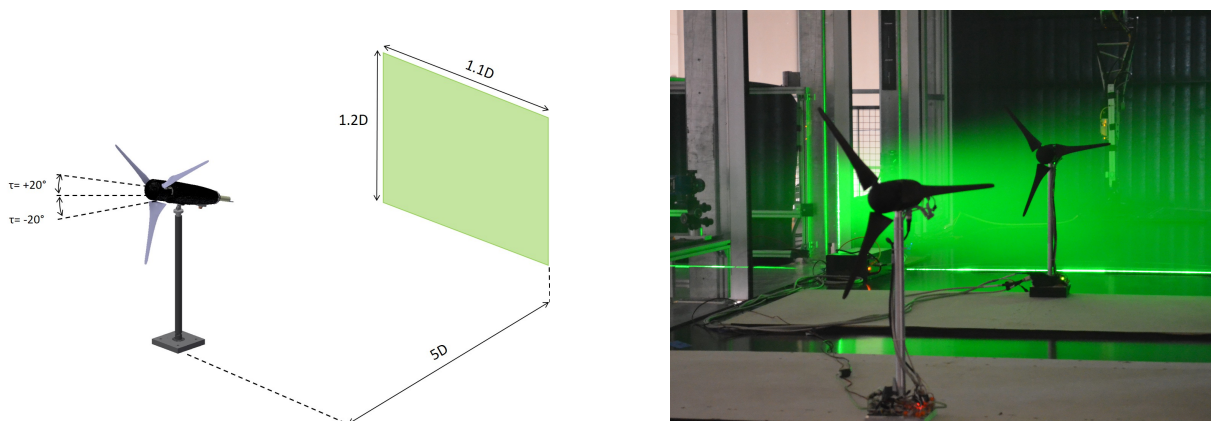


Figure 4: Sketch of the experimental set-up showing the wind turbine model and the measuring S-PIV plane (left) and photo of the UTD BLAST wind tunnel test section with the two scaled wind turbines installed (right).

will be used for validation of CFD simulations that, at later stage, will expand this study further downstream.

First, the power output of the turbines was measured for three tilt angles of the upstream rotor, namely $\tau = 0^\circ$ (aligned), $\tau = 20^\circ$ (backward tilt) and $\tau = -20^\circ$ (forward tilt). The tilting of the rotor was achieved through a hinge placed between the nacelle and the tower, which can be adjusted manually prior to the experiment. Since the hinge is below the rotor axis, a negative tilt (downward wake deflection) implies a lowering of the rotor, and the opposite for a positive tilt. Next, the downstream wind turbine was removed and the velocity field was measured using S-PIV at a crossplane coinciding with the downstream rotor location, i.e. 5 diameters downstream of the first wind turbine (Fig. 4). For the S-PIV measurements a complete LaVision system was

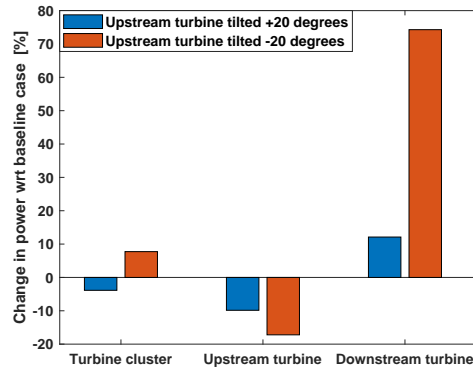


Figure 5: Power production changes, relative to the baseline case, for the cluster of two turbines.

used, which comprised of two sCMOS 5.5 Mp cameras mounted on Scheimpflug adapters and equipped with 50 mm Nikon AF 1.8D lenses. A Quantel Evergreen HP laser was used with a 380 mJ/pulse. For the calibration of the cameras, a 300×300 mm dual-plane calibration target was used. Using the pinhole calibration technique the field of view (FOV) was approximately 0.7×0.8 m. For each test condition, 2000 image pairs were acquired at a 10 Hz frequency. A sensitivity analysis demonstrated convergence of the flow statistics.

Figure 5 shows the effect on power production (relative to the baseline case) for the cluster of the two turbines. The data was obtained directly from the onboard sensors of the scaled wind turbines. Results show that the effect of tilt on the power of both machines is asymmetrical for negative and positive tilt angles, even though this trend is much more evident for the downstream machine. In addition, there is an advantage for total power production when the wake is deflected towards the ground. The reason for this lies in the vertical displacement of the wake in conjunction with the non-uniformity of the incoming flow due to the presence of the boundary layer. When the wake is deflected upwards, its space is occupied by the flow close to the ground, which is of a relatively low kinetic energy. Conversely, when the wake is deflected towards the ground, higher energy flow entrains the rotor area of the downstream machine. This can be seen in Fig. 6, which shows contours of normalized streamwise velocity u/U_o for the baseline case, $\tau = -20^\circ$ and $\tau = +20^\circ$ at a vertical plane that coincides with the downstream rotor position. The vertical deflection of the wake is evident for the cases with the tilted upstream rotor. Additionally, it can be observed that a downward deflection of the wake results in a considerable part of the downstream rotor operating outside the wake of the front turbine, which explains its better power performance for this condition. Regarding the upstream machine, the difference between negative and positive tilt angles can be also attributed to the presence of the boundary layer: tilting the rotor results also in a non-negligible vertical translation of the rotor. Hence, when the rotor is, for instance, tilted 20° (upward wake deflection) it is also displaced $0.1D$ up, towards higher wind speed. Assuming that the center of floatation is below the rotor axis, this effect will be also present (at least in trend, if not in exact value) in the full scale offshore platform case. The effect of the tilt direction on the total power gain presented here agrees well with the results reported in [2].

Figure 7 shows a map of the turbulence intensity $TI = \overline{U}/\sigma$; Fig. 8 shows maps of the added turbulence intensity, which is defined as follows:

$$T I_{u,add} = +\sqrt{T I_u^2 - T I_{u,inflow}^2} \quad T I_u \geq T I_{u,inflow}, \quad (1a)$$

$$T I_{u,add} = -\sqrt{T I_{u,inflow}^2 - T I_u^2} \quad T I_u < T I_{u,inflow}. \quad (1b)$$

The figures reveal that the turbulence intensity experienced by the downstream rotor changes drastically when the upstream rotor tilts. Looking at the map for zero tilt reported in Fig. 7 (left), it can be seen that the turbulence intensity within the wake has a horseshoe shape, which agrees with what is reported in [9]. The change in turbulence intensity is the result of two opposite effects that a rotor has on a boundary-layer inflow: on the one hand the breakdown of the wake structures increases turbulence intensity, and on the other hand the velocity deficit induced by the rotor results (in some parts of the wake) in a smaller vertical shear, which reduces turbulence intensity. This can be seen in Fig. 8 (left), where in the lower part of rotor disk area the added turbulence intensity is negative. When the wake is deflected towards the sky, the ambient vertical shear is reduced in a greater portion of the rotor disk area. Therefore, the region of negative added turbulence intensity that the downstream rotor experiences is increased, as Fig. 8 (center) suggests. In parallel, the upper region of the wake, where turbulence intensity increases, is pushed out of the rotor disk. When the wake is deflected towards the ground, Fig. 7 (right) shows that the horseshoe shape has practically vanished. The upper, high turbulence intensity part of the wake has moved to the center of the rotor disk area and, consequently, a free stream flow of high velocity and relatively low turbulence intensity has occupied this region. Integrating the turbulence intensity over the rotor disk area, in the upward deflection case the turbulence intensity area integral is 16% lower than in the zero tilt case, while for the downward deflection case it is 4% lower.

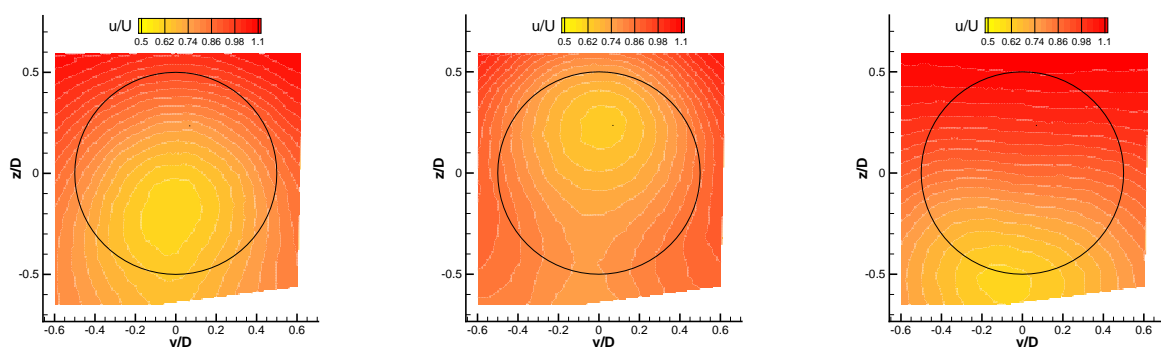


Figure 6: Normalized streamwise velocity contours for tilt angles $\tau = 0^\circ$ (left), $\tau = +20^\circ$ (center) and $\tau = -20^\circ$ (right). The black circle represents the rotor disk perimeter.

3.2. LES simulations

CFD simulations of the experimental set-up were ran using an LES flow solver based on Foam-extend [10], while the wind turbine was modeled in FAST [11]. This framework has been validated in previous work [12]. The aim in the present paper is mainly to validate the CFD simulations against the experimental data and, at a second stage, to extend the study to tilt angles and downstream distances beyond the available experimental data. The results of these CFD simulations are, unfortunately, not yet available at the time of writing. Figure 9 shows the

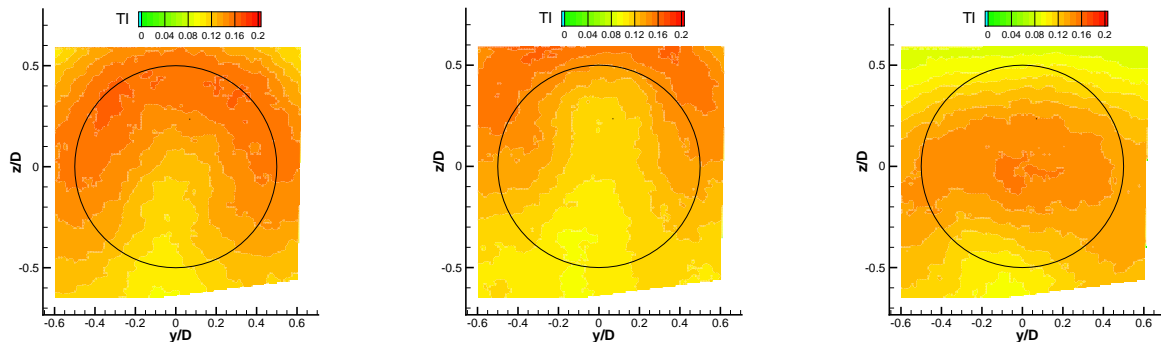


Figure 7: Turbulence intensity contours for tilt angles $\tau = 0^\circ$ (*left*), $\tau = +20^\circ$ (*center*) and $\tau = -20^\circ$ (*right*). The black circle represents the rotor disk perimeter.

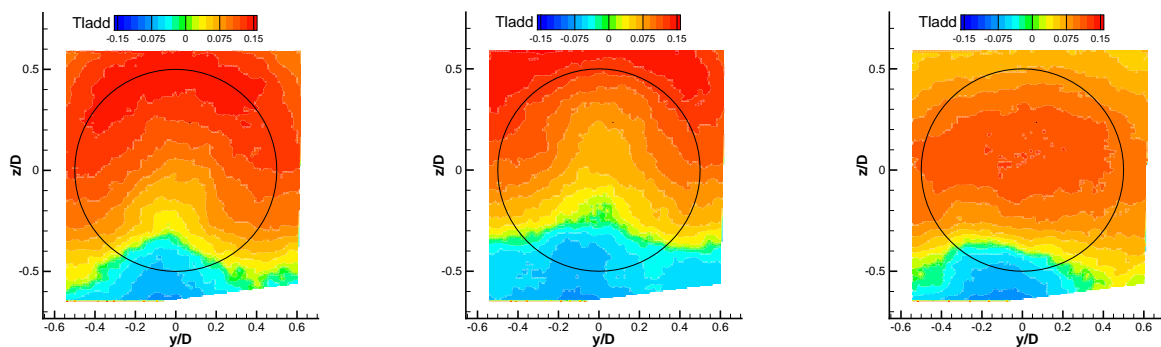


Figure 8: Added turbulence intensity contours for tilt angles $\tau = 0^\circ$ (*left*), $\tau = +20^\circ$ (*center*) and $\tau = -20^\circ$ (*right*). The black circle represents the rotor disk perimeter.

percent error of the streamwise velocity between experiment and CFD (the error being defined as $\epsilon = (U_{exp} - U_{cfd})/U_{exp}$). The comparison shows good agreement, since the maximum error is around 5% and only in small regions for the aligned case. For the upward and downward deflection case the agreement is even better with the maximum error being below 4%.

Figure 10 shows individual and cluster power changes with respect to the upstream rotor tilt angle, compared to the baseline non-tilted case. The power change for the downstream machine was calculated, for both experiment and CFD, based on the integral of the wind speed over the rotor disk area. The power change for the upstream machine is measured (for the experiment) or obtained directly from FAST (for the CFD). The minimum of the downstream machine power change is not at 0° tilt, which is to be expected since the wake for the aligned case (due to the interaction with the non-uniform inflow) is moved towards the ground by approximately $0.2D$. The same phenomenon can be observed for the upstream machine curve and, as explained above, it is due to the vertical translation of the rotor that is associated with the tilting. The curve of the cluster power change is almost linear, resulting in a power increase of about 5%. This is less than the 8% that was measured directly from the sensors installed on the turbines. However, the available numerical and experimental data do not allow for solid conclusions regarding the nature of this discrepancy, which, in any case, does not question the observed trend.

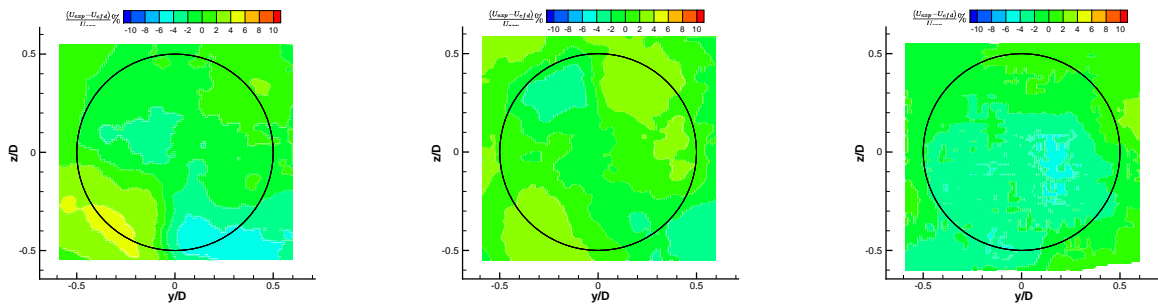


Figure 9: Percent error between experimental and CFD results for $\tau = 0^\circ$ (*left*), $\tau = +20^\circ$ (*center*) and $\tau = -20^\circ$ (*right*) at a crossplane $5D$ downstream the rotor. The black circle represents the rotor disk perimeter.

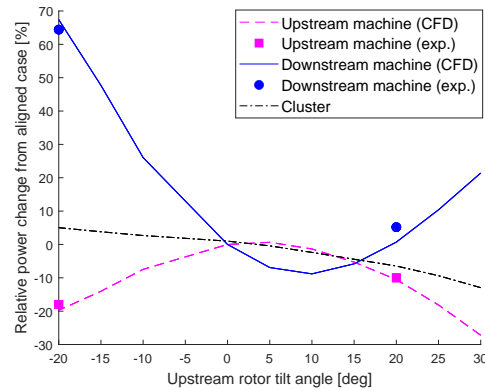


Figure 10: Power production changes, relative to the baseline case, for the individual turbines and the cluster.

4. Conclusions

This article is a preliminary look into the feasibility of using active ballast control for vertically redirecting the wake of offshore wind turbines. Simple calculations on a semi-submersible foundation concept show that this control method is relatively slow (1 min/deg), yet feasible without the need for radical redesigns.

Both numerical and experimental results showed that redirection of the wake towards the sea surface has a positive effect on the power production of the cluster, while deflecting the wake towards the sky has a negative effect. On the other end, deflecting the wake towards the sky led to a substantially lower turbulence intensity for the downstream machine. A similar, but less strong, effect was observed when the wake was deflected towards the ground. The vertical deflection effectiveness and its influence on wake behavior can be substantially affected by the tilting geometry (for example, in terms of vertical translation associated with tilting) and the boundary layer profile.

One major limit of this study is that, although it shows trends and reveals some of the acting mechanisms of vertical wake deflection, it was performed for $5D$ turbine spacing, which is not representative of offshore conditions. This topic is the focus of ongoing investigations. Additional future work will also consider the use of vertical wake deflection control per se, as well as its integration with lateral wake control.

4.1. Acknowledgments

The authors would like to thank Dr. Kyle Jones for his contribution to the execution of the experiments and the post processing of the experimental data, along with Dr. Antonis Daskalakis for his advice on the balast control calculations. The authors also express their appreciation to the Leibniz Supercomputing Centre (LRZ) for providing access and computing time on the SuperMUC Petascale System.

References

- [1] Campagnolo F, Petrović V, Schreiber J, Nanos E M, Croce A, and Bottasso C L 2016 Wind tunnel testing of a closed-loop wake deflection controller for wind farm power maximization *Journal of Physics: Conference Series* **753** .
- [2] Annoni J, Scholbrock A, Churchfield M and Fleming P 2017 *Evaluating Tilt for Wind Plants* American Control Conference Seattle 717-22.
- [3] Srinivas G, Troldborg N, and Gaunaa M 2012 *Application of engineering models to predict wake deflection due to a tilted wind turbine* European Wind Energy Conference and Exhibition.
- [4] Roddier D, Cermelli C and Weinstein A 2009 *Windfloat: A Floating Foundation for Offshore Wind Turbines Part I: Design Basis and Qualification Process* Proc. of the ASME 2009 28th Int. Conf. on Ocean Honolulu.
- [5] <https://questfwe.com/about-us/>
- [6] Liu Y, Li S, Yi Q and Chen D 2016 Developments in semi-submersible floating foundations supporting wind turbines: A comprehensive review *Renewable and Sustainable Energy Reviews* **60** 433449.
- [7] Diaz P et al. 2012 *Offshore vertical wind shear: Final report on NORSEWinDs work task 3.1* DTU Wind Energy E, No. 0005
- [8] Nanos E M, Kheirallah N, Campagnolo F and Bottasso C L Design of a multipurpose scaled wind turbine model *Journal of Physics: Conference Series* **1037** .
- [9] Bastankhah M and Porté -Agel F 2017 A new miniature wind turbine for wind tunnel experiments. Part II: Wake Structure and Flow Dynamics *Energies* **10** 923.
- [10] Jasak H 2009 OpenFoam: open source CFD in research and industry *Int. Nav. Arch. Ocean* **1** 89.
- [11] Guntur S, Jonkman J, et al. 2016 FAST v8 verification and validation for a MW-scale wind turbine with aeroelastically tailored blades *Wind Energy Symp.*
- [12] Wang J, et al. 2019 Wake behavior and control: comparison of LES simulations and wind tunnel measurements *Wind Energy Sci.***4**(1) 71-88.